Advances in Adaptive Data Analysis
Vol. 2, No. 4 (2010) 397–414

DOI: 10.1142/S1793536910000604

World Scientific
www.worldscientific.com

# ON THE FILTERING PROPERTIES OF THE EMPIRICAL MODE DECOMPOSITION

ZHAOHUA WU*

*Department of Earth, Ocean and Atmospheric Science &*
*Center for Ocean-Atmospheric Prediction Studies,*
*Florida State University, Tallahassee, FL 32306, USA*
*zwu@fsu.edu*

NORDEN E. HUANG

*Research Center for Adaptive Data Analysis,*
*National Central University, Chungli, Taiwan 32001, ROC*

The empirical mode decomposition (EMD) based time-frequency analysis has been used in many scientific and engineering fields. The mathematical expression of EMD in the time-frequency-energy domain appears to be a generalization of the Fourier transform (FT), which leads to the speculation that the latter may be a special case of the former. On the other hand, the EMD is also known to behave like a dyadic filter bank when used to decompose white noise. These two observations seem to contradict each other.

In this paper, we study the filtering properties of EMD, as its sifting number changes. Based on numerical results of the decompositions using EMD of a delta function and white noise, we conjecture that, as the (pre-assigned and fixed) sifting number is changed from a small number to infinity, the EMD corresponds to filter banks with a filtering ratio that changes accordingly from 2 (dyadic) to 1; the filter window does not narrow accordingly, as the sifting number increases. It is also demonstrated that the components of a delta function resulted from EMD with any prescribed sifting number can be rescaled to a single shape, a result similar to that from wavelet decomposition, although the shape changes, as the sifting number changes. These results will lead to further understandings of the relations of EMD to wavelet decomposition and FT.

*Keywords*: Time-frequency analysis; Fourier transform; wavelet decomposition; empirical mode decomposition; ensemble empirical mode decomposition; intrinsic mode function; sifting process; sifting stoppage criteria; filter banks.

## 1. Introduction

The empirical mode decomposition (EMD) based time-frequency analysis method, first proposed by Huang and his colleagues [Huang *et al.* (1998)] and later improved by many researchers [Huang *et al.* (1999); Huang *et al.* (2003); Rilling *et al.* (2003); Huang *et al.* (2009); Wu and Huang (2004, 2005, 2009); Wu *et al.* (2007, 2009)], has emerged as a popular method in time series analysis and signal processing fields.

*Corresponding author.

It has found many applications in many scientific and engineering fields [Huang and Attoh-Okine (2005); Huang and Shen (2005); Huang and Wu (2008)]. The EMD is a temporally local and adaptive analysis method that reveals well the nonlinear nonstationary nature of physics hidden in data. Contrary to most time-frequency analysis tools, the EMD is a method that needs neither any *a priori* bases nor stationary assumption (see Sec. 2 for more details).

The EMD is an algorithm without a definite analytical expression; the understanding of its mathematical properties so far is gained mostly through numerical expressions. In the last few years, some intriguing properties of EMD have been revealed. For example, the EMD behaves like a dyadic filtering bank for a large class of noise [Rilling *et al.* (2003); Flandrin and Gonçalves (2004); Wang *et al.* (2010)] and for the delta function [Huang *et al.* (1998); Flandrin *et al.* (2004)]; moreover, in these cases, the Fourier spectra of all the components collapse to a single shape when viewed as function (PDF) of the logarithm of frequency and their amplitudes are appropriately rescaled. The probability density function (PDF) of a single component of noise resulting from EMD is approximately a Gaussian distribution, which can be inferred from the central limit theorem [Wu and Huang (2004, 2005)]. These interesting properties of EMD also led to the development of a method that determines whether or not an oscillatory component (called an intrinsic mode function (IMF)) of any give time series can be statistically distinguished from any component of a white noise series [Wu and Huang (2004, 2005)].

Since EMD is a time-frequency analysis method, many researches wonder whether or not EMD is related to the well-studied Fourier transform (FT) and wavelet analysis. Indeed, some intriguing relations have been revealed. For example, all the IMFs of a delta function resemble the cubic spline wavelet [Flandrin and Gonçalves (2004); Flandrin *et al.* (2005)] and collapse to a single shape (a cubic spline-like wavelet) with appropriate scaling. Another interesting example is that two sinusoidal waves of the same amplitude but with minor difference in frequency can be cleanly separated when their sum is decomposed using EMD with a large sifting number [Huang *et al.* (1998)], (see more details in Sec. 2). This latter result seems to contradict the dyadic filter property mentioned earlier.

To reconcile these observed yet seemingly contradictory properties of EMD and to explore the relations of EMD to the FT and wavelet decomposition, we will further investigate properties of EMD in this study, emphasizing the changing properties as the sifting number changes. In Sec. 2, we review EMD and its more recent improvement, the ensemble EMD (EEMD), which uses noise to assist the decomposition of data so as to obtain more physically meaningful and robust components [Wu and Huang (2008)]; we also illustrate what leads to the apparent contradictory properties of EMD. In Sec. 3, we examine numerically how the change of sifting number causes the filtering properties of EMD and propose a conjecture regarding EMD filtering properties based on the numerical results. In Sec. 4, we illustrate how EMD can be regarded as a generalization of wavelet analysis in the special case of

a delta function and how the EMD components share the constant amplitudes with FT in the decomposition of white noise. A summary and discussion is presented in Sec. 5.

## 2. The Empirical Mode Decomposition

### 2.1. *The EMD algorithm*

The detailed description of the EMD method can be found in Huang *et al.* (1998) and Huang *et al.* (1999). In contrast to most previous methods of data analysis, the EMD method is adaptive and temporally local, with the basis of the decomposition derived from the data. In EMD, the data $x(t)$ is decomposed in terms of the IMFs, $c_j$, which is defined as any functions having the same numbers (or at most differing by one) of zero-crossings and extrema, and also having symmetric envelopes. In mathematical terms, $x(t)$ is expressed as,

$$x(t) = \sum_{j=1}^{n} c_j(t) + r_n(t), \tag{1}$$

where

$$c_j(t) = a_j(t) \cos\left[\int \omega_j(t)dt\right], \tag{2}$$

and $r_n$ is the residual of the data $x(t)$, after $n$ IMFs are extracted.

In practice, EMD is implemented through a sifting process that uses only local extrema. From any dataset $r_{j-1}$, say, the procedure is as follows: (1) identify all the local extrema (the combination of both maxima and minima) and connect all these local maxima (minima) with a cubic spline as the upper (lower) envelope; (2) obtain the first component $h$ by taking the difference between the data and the local mean of the two envelopes; and (3) treat $h$ as the data and repeat Steps 1 and 2 as many times as is required until the envelopes are considered symmetric with respect to zero mean under *a prescribed criterion*. The final $h$ is designated as $c_j$. A complete sifting process stops when the residue, $r_n$, becomes a monotonic function or a function containing only one internal extremum from which no more IMF can be extracted. Following this algorithm, the IMFs expressed in Eq. (2) are simple oscillatory functions with relatively slow varying and nonnegative amplitude and relatively fast-changing and nonnegative frequency at any temporal location.

The EMD has some unique properties. It is a temporally local analysis method [Huang and Wu (2008); Wu and Huang (2009)]. It behaves as a dyadic filter bank in which the Fourier spectra of various IMFs collapse to a single shape when rescaled appropriately [Flandrin *et al.* (2004); Wu and Huang (2004, 2005)]. For a time series with length $N$, the commonly used EMD algorithm usually results in close to but no more than $\log_2 N$ components. Such a sparse decomposition method often improves the efficiency in representing signals of data.

Even though EMD has these wonderful properties, it also has a serious "mode (scale) mixing" problem, which manifests itself in IMFs consisting of oscillations

of dramatically disparate scales. An annoying implication of such mode mixing is related to lack of stability and lack of the "physical uniqueness" of the EMD decomposition. Real data almost always contain a certain amount of random noise or intermittences that is not explicitly known to us, it is thus important to gauge to what extent a decomposition algorithm leads to results that are sensitive to noise. If the decomposition is insensitive to added noise of small but finite amplitude and suffers little quantitative and no qualitative change, the decomposition is generally considered stable and satisfies the "physical uniqueness" criterion; otherwise, the decomposition is unstable and does not satisfy the physical uniqueness. In the latter case, the decomposition may not be reliable and may not be suitable for physical interpretation. Unfortunately, EMD in general does not satisfy this stability requirement due its being solely based on the distribution of extrema.

To solve this problem, the EEMD was developed by [Wu and Huang (2009)]. In this method, counter-intuitively, multiple noise realizations are added to one-time series of observations to mimic, from a single observation, a scenario of multiple trials of observation so as to carry out an ensemble average approach for the corresponding IMFs and extract scale-consistent signals. The major steps of the EEMD method are as the following:

(1) add a white noise series to the targeted data;
(2) decompose the data with added white noise into IMFs;
(3) repeat Steps 1 and 2 again and again, but with different white noise series each time; and
(4) obtain the (ensemble) means of corresponding IMFs of the decompositions as the final result.

Heuristically, the effects of the added white noise series cancel each other in the ensemble average, and the mean IMFs stay within the natural dyadic filter windows as discussed in Flandrin *et al.* (2004) and Wu and Huang (2004, 2005), significantly reducing mode (scale) mixing. The role of the added noise in the EEMD is similar to that of a catalyst in a chemical reaction, not participate in the end results of the reaction but facilitating the reaction. Therefore, the EEMD is a truly *noise-assisted data analysis* method and keeps the "physical uniqueness." Since the EEMD is based on the EMD method, the former's adaptiveness and the temporal locality are preserved, making it an effective method consistent with the physical data analysis.

### 2.2. *Effect of continuing sifting*

Although EMD and its major variation and the EEMD have been demonstrated useful in many applications, the empirical nature of the method has left many crucial questions unanswered. One of them is the stoppage criterion corresponding to the approximate symmetry of upper and lower envelopes for stopping further sifting. By far, commonly used stoppage criteria include (1) a Cauchy type criterion

[Huang *et al.* (1998)] and its variations [Shen *et al.* (2005)]; (2) S-number criterion [Huang *et al.* (2003)]; (3) combined global-local stoppage criterion [Rilling *et al.* (2003)]; and (4) fixed sifting number criterion [Wu and Huang (2004, 2005, 2009)]. It should be noted that all these criteria are largely determined based on, without any strong theoretical bases, individual researchers' experience of using the EMD in their research. It is also noteworthy that almost all previous studies, if tracking the sifting numbers in the decomposition processes, lead one to observe that the sifting numbers are often less than 100.

It is thus natural to ask what the effect is of continuing sifting. To answer this question in full generality may be out of our reach. However, the qualitative effect of sifting can be illustrated through the decomposition of a synthetic signal

$$y(t) = \left[1 + 0.5\cos\left(\frac{2\pi t}{5}\right)\right]\sin(2\pi t). \tag{3}$$

$y(t)$ satisfies the definition of an IMF with analytically symmetric upper and lower envelopes with respect to zero mean, and it is displayed Fig. 1.

The result presented in Fig. 1 show that when the sifting number is increased continuously, the amplitude modulation of the IMF becomes less pronounced, and eventually the amplitude becomes a constant. This result is understandable: for an amplitude-frequency modulated mono-component, the exact local amplitude

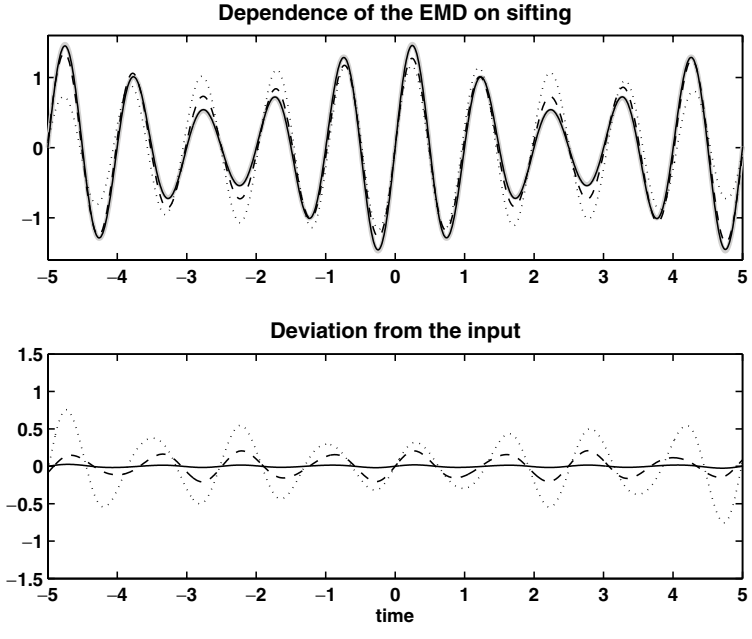


Fig. 1. The effect of further sifting of an analytically well-defined IMF expressed by Eq. (3). The bold gray line in the upper panel is the synthetic signal. The thin solid, dashed, and dotted lines in the upper (lower) panels are the sifting results (differences of the synthetic signal and sifting results) with sifting number $2^3, 2^8$, and $2^{13}$ times, respectively.

between neighboring maxima (minima) may not be expressed by any low-order polynomials or splines that pass through these maxima (minima). In the EMD, only extrema information is used to obtain an envelope (amplitude) approximation to the unknown true envelope, and it is thus inevitable that the envelope obtained from this extrema information is a distorted and often smoothed version of the unknown true envelope. In such a case, since a maximum and a minimum of a signal cannot appear at the same temporal location, the upper and lower envelopes of the sifting process of an analytically exact IMF may fail to be symmetric with respect to zero mean, introducing a bias, albeit small, in the estimation of the supposed zero mean reference. Therefore, as further sifting is carried out to satisfy the requirement of envelopes being symmetric with respect to zero line, the amplitudes of IMFs of any given data in EMD will degenerate to a straight line. A proof of such sifting effect is presented in the appendix, which closely follows the proof of Wang *et al.* (2010). It should be noted here that, in general, the excessive sifting only flattens the amplitude but does not change noticeably the frequency for an amplitude-frequency modulated mono-component: the total number of extrema of an IMF is likely to remain a constant or to undergo almost a very small relative change. It can be demonstrated numerically that this also holds for any amplitude-frequency modulated IMF.

### 2.3. *EMD as a dyadic filter or a nondyadic filter*

The $x(t)$ in Eqs. (1) and (2) decomposed using the FT would be

$$x(t) = \mathrm{Re} \sum_{j=1}^{N} a_j e^{i\omega_j t}, \tag{4}$$

with both $a_j$ and $\omega_j$ as constants.

The similarity between Eqs. (4) and (2) is clear: the mathematical expression of the EMD appears to be a generalized form of that of FT, which leads to the speculation that FT may be a special case of EMD with constant amplitude and frequency. Indeed, this speculation was supported by an unambiguous but often ignored example in Huang *et al.* (1998). In that example, the sum of two unit amplitude sinusoidal waves with close constant frequencies was decomposed using EMD with a sifting number of 3000, the two sinusoidal waves were qualitatively separated. A similar example is displayed in Fig. 2. To further illustrate how the change of the sifting number can change the results of the decomposition, we present in Fig. 2 decompositions of the synthetic data in Huang *et al.* (1998) with sifting numbers of 10, 1000, and 100000. It is clear that when the sifting number is small, the synthetic signal is considered essentially as an amplitude modulated wave with a frequency that is the mean frequency of the prescribed sinusoidal waves. As the sifting number becomes larger and larger, the amplitude modulation is smoothed and eventually disappears.

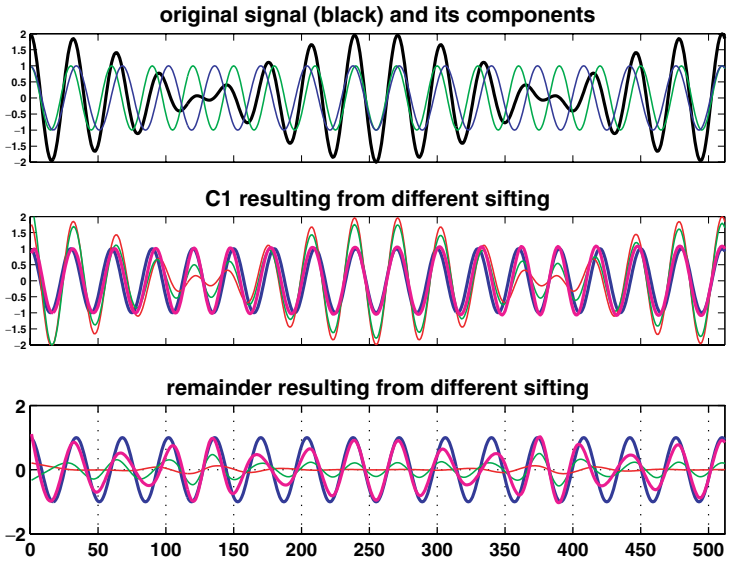


Fig. 2. Upper panel: a signal (bold black line) composed of two unit amplitude sinusoidal waves with periods of 30 (thin blue line) and 34 (thin green line), respectively. The decompositions of the signal with different sifting numbers are displayed in the middle (the first IMF) and lower (the remainder) panels. The red, green, and magenta lines in the middle and lower panels are the components corresponding to sifting numbers of 10, 1000, and 100000, respectively. The blue lines in the middle and lower panels correspond to the shorter period (30) waves and longer period (34) waves in the upper panel, respectively.

The filtering property illustrated in the above example shows that EMD is capable of separating two sinusoidal waves of small frequency difference. However, other studies [Flandrin *et al.* (2004, 2005); Wu and Huang (2004, 2005)] have shown that EMD behaves approximately as a dyadic filter bank when used to "decompose" noise, although the exact filtering ratio varies, e.g., the ratio is almost exact 2 in Wu *et al.* (2004) and 1.83 in Flandrin *et al.* (2005). This notion of EMD as a dyadic filter bank has been widely accepted. It is thus a natural question whether EMD is a dyadic filter bank or a nondyadic filter bank that can separate components of small frequency difference.

Before we answer this question in detail in the next section, we would like to point out that the contradiction of filtering properties of EMD may be only apparent. The notion of EMD as a dyadic filter bank resulted mostly from studies in which the actual sifting numbers for the decompositions were often of the order of 100 or smaller. However, in the example of the decomposition of two sinusoidal waves with very small frequency change, a quality decomposition of the two waves is obtained only of the sifting number is very large. Indeed, the characteristics of EMD with large sifting numbers have not been systematically investigated.

## 3. Ratio of the EMD Filter Banks

In this section, we examine numerically how the filtering properties of EMD changes as the sifting number in EMD changes. The quantitative results of the observed filtering properties may vary when the EMD is applied to different time series, but we expect the qualitative results described in what follow to hold for any time series. To illustrate these properties, we present the decomposition results only for the delta function and white noise, two typical types of data that have been widely studied by many time-frequency analysis methods.

### 3.1. *Decompositions of delta function*

The decomposition of the delta function was seen in various publications (Flandrin and Gonçalves, 2004; Flandrin *et al.*, 2005). Since the delta function has only one extremum, the direct decomposition using EMD is not feasible. To avoid this difficulty, in practice one adds a very small amplitude white noise to the delta function and decomposes the noise-added delta function. However, since the distribution of extrema along the temporal axis of the noise-added delta function is not identical for different realizations of the small amplitude noise, the decompositions of delta function with different realizations of noise series added may result in significantly different results. To overcome this drawback, an ensemble approach is adopted in Flandrin and Gonçalves (2004) and Flandrin *et al.* (2005): taking the averages of the same rank IMFs from different noise-added delta functions with different noise series realizations. In this way, it is found in Flandrin and Gonçalves (2004) and Flandrin *et al.* (2005) that all IMFs of a delta function satisfy

$$C_k(n) = \frac{1}{\alpha^k}\psi\left(\frac{n}{\alpha^k}\right), \tag{5}$$

where $C_k$ is the $k$th IMF; $n$ is the data location of a discrete time series with length $N$; $\psi$ has a certain shape (resembling the cubic spline wavelet in Flandrin and Gonçalves (2004) and Flandrin *et al.* (2005)) and $\alpha$ is a scale factor 1.83 in Flandrin and Gonçalves (2004) and Flandrin *et al.* (2005).

Figure 3 displays the decompositions of delta functions with fixed sifting numbers of 10 and 2500, respectively. Figure 4 displays the rescaled IMFs for both cases. The two decompositions of the delta function are qualitatively different. In the case of a small sifting number (fixed to 10), the EMD behaves like a cubic spline wavelet transform with a scale factor of 2. However, for the case of a relatively large sifting number (equal to 2,500), the IMFs no longer resemble cubic spline wavelet, rather, they show more visually identifiable extrema (7) than that of a cubic spline wavelet (6). All the IMFs still have approximately the same shape when they are rescaled with a scale factor 1.32. In addition to these differences, the amplitude difference between the neighboring maxima in each IMF is smaller, indicating amplitude flattening. As the sifting number continues to increase, the scale factor becomes smaller; more extrema in the IMF appear; the difference of

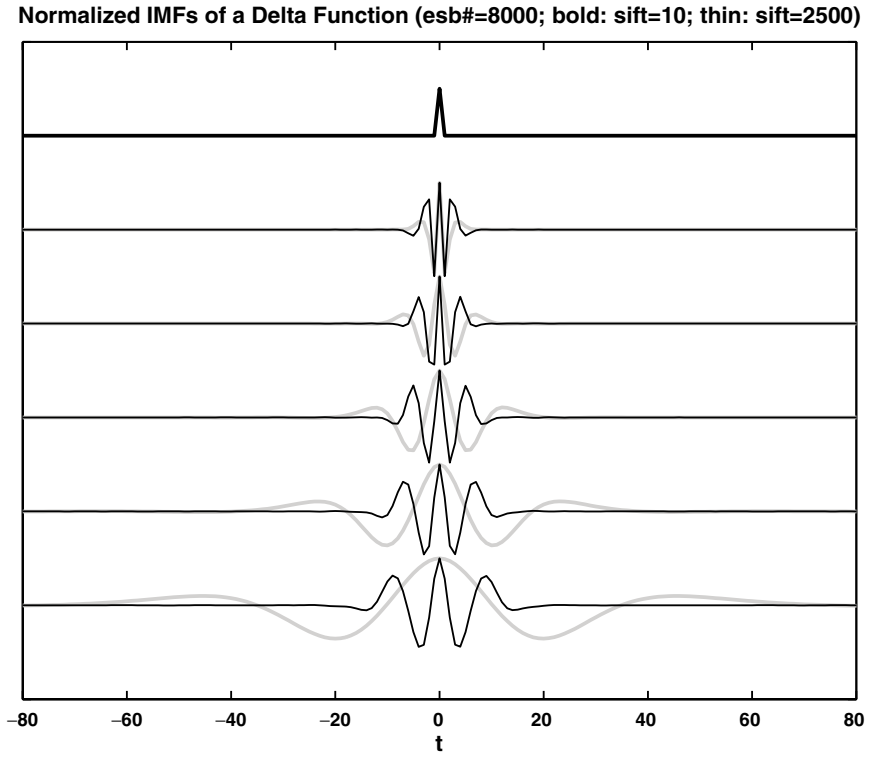


Fig. 3. Decompositions of delta function using different sifting numbers. The thick black line at the top is the given delta function; the thin black and solid gray lines are IMFs from the decompositions with sifting number 10 and 2500, respectively. In this figure, the delta function and each IMF are normalized by their maximum values, respectively.

amplitude between neighboring maxima (minima) becomes smaller; and the scale factor approaches 1.

From Eq. (6), it is inferred that the amplitude $A_k$ and the mean energy $E_k$ of $k$th IMF of a delta function should satisfy the following relations

$$\frac{A_k}{A_{k+1}} = \alpha \quad \text{and} \quad \frac{E_k}{E_{k+1}} = \alpha, \tag{6}$$

where $A_k$ is the maximum absolute value of $k$th IMF, and $E_k$ is defined as

$$E_k = \frac{1}{N}\sum_{n=0}^{N} C_k^2(t_n). \tag{7}$$

If logarithms of amplitude and the mean energy for all IMFs are plotted, both of them should be straight lines. This result is confirmed in Fig. 5 although the amplitude and the mean energy of an IMF may deviate a little bit from the straight lines. The slopes of the straight lines of the logarithms of amplitude and the mean energy also help to determine the scaling factors.

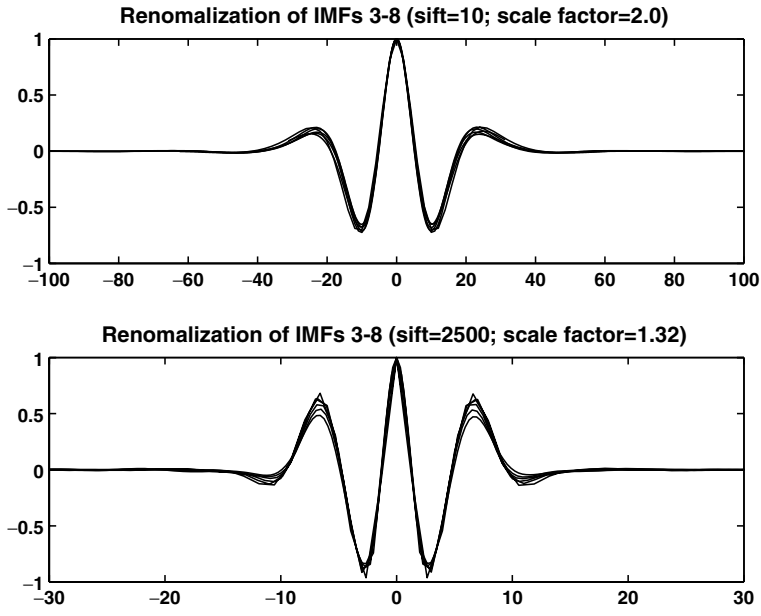


Fig. 4. The rescaled IMFs 3–8 of the decompositions of delta function with a sifting number 10 (upper panel) and 2500 (lower penal), respectively. The reference IMFs (without rescaling) in both cases are the corresponding fourth IMF.

### 3.2. *Decompositions of white noise*

The decomposition of white noise was reported in Flandrin *et al.* (2004) and Wu and Huang (2004, 2005). Since the characteristics of a short realization of a white noise series can appear different from these of other realizations of the same length, to obtain general characteristics, a white noise series of $2^{16}$ data points are decomposed. The sifting number used in these decompositions $2^m$, with $m = 3, \ldots, 16$.

A randomly selected section of 256 data points of the decomposition of the lengthy white noise series is displayed in Figs. 6 and 7, for sifting numbers $2^3$ and $2^{12}$, respectively. The difference of the decompositions with different sifting number is visually clear. Generally speaking, the IMFs for the small sifting number have relatively fast modulation of amplitude; and the average of periods (defined as the distances between neighboring maxima) of neighboring IMFs are about doubled as reported in [Flandrin *et al.* (2004); Wang *et al.* (2010); Wu and Huang (2004)]. Each IMF still contains a high degree of amplitude and frequency modulation. For the large sifting number, we have more IMF components. Furthermore, the amplitudes of IMFs contain only very low-frequency variability or are even flattened; although the irregularity is much reduced in amplitude, it is largely retained in the frequency modulation. In addition to these differences, the average periods of neighboring IMFs become closer in EMD with larger sifting numbers. The trend of amplitude and frequency variation as a function of the sifting number suggests that

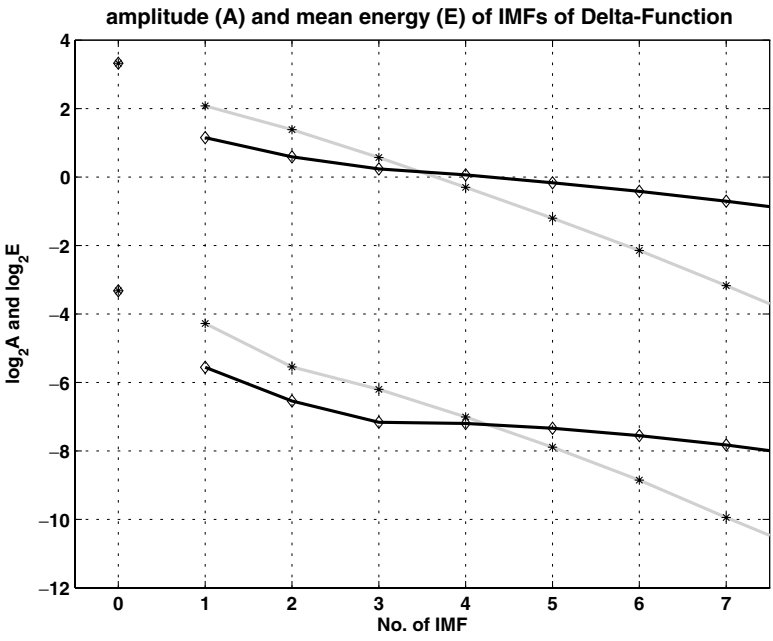


Fig. 5. The logarithms of amplitude and the mean energy of the delta function and its IMFs. The upper (lower) groups of asterisks except the first from the left are the amplitude (mean energy) for the case of a small sifting number 10; and the upper (lower) groups of diamonds except the first from the left are the amplitude (mean energy) for the case of a large sifting number 2500. The bold lines have no meaning but are used to guide how close they are to a straight line. The integer value along the horizontal axis is the order of IMF, with a value $k$ corresponding to $k$th IMF. The amplitude of the delta function and its mean energy are also plotted the vertical line with its value zero at the horizontal axis.

as the sifting number increases, the amplitudes would become uniform with only the frequency retaining some modulation. This happens despite the randomness inherent to the original data.

As observed in Flandrin *et al.* (2004) and Wu and Huang (2004, 2005), the averaged ratio of the mean periods of the neighboring IMFs of white noise is a constant, approximately 2 for the small sifting number they used. It is legitimate to wonder whether or not such a constant ratio will appear in other decompositions with a fixed sifting number. Figure 8 presents the ratios of the mean periods, $\overline{T}_{k+1}/\overline{T}_k$, with $\overline{T}_k$ and $\overline{T}_{k+1}$ the mean periods of the $k$th and $(k+1)$th IMFs, respectively, for decompositions with various sifting numbers of $2^m, m = 3, \ldots, 16$. From the results displayed, it is clear that a constant mean period ratio holds nicely, although not exactly, for any decomposition with a fixed sifting number. When the sifting number is $2^3$, the averaged ratio is slightly over 2. This ratio decreases as the sifting number increases. It is about 1.44 for the case of a sifting number of $2^{12}$, and about 1.35 for the case of a sifting number of $2^{16}$. An apparent feature of the ratio is its decrement slows down, as the sifting number is continuously doubled.

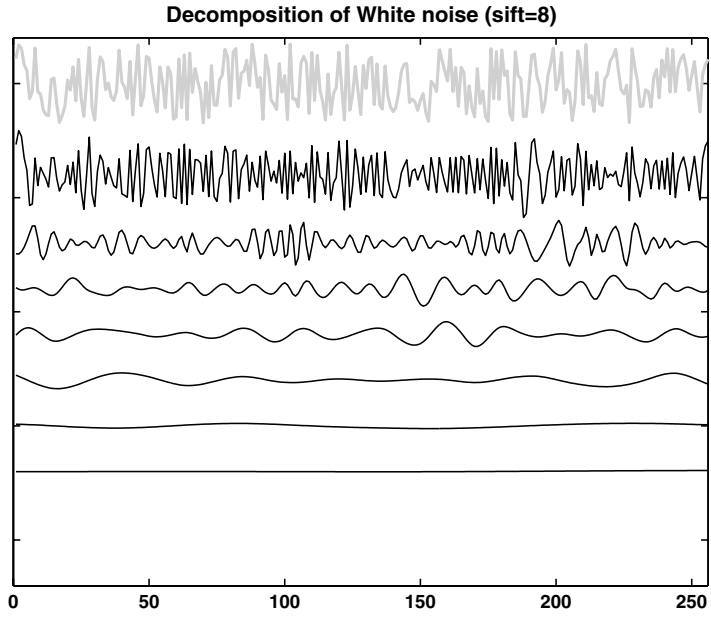


Fig. 6. Decomposition of a white noise series using EMD with a sifting number 8. The gray line is the original white noise and the black lines are the IMFs of this time series.

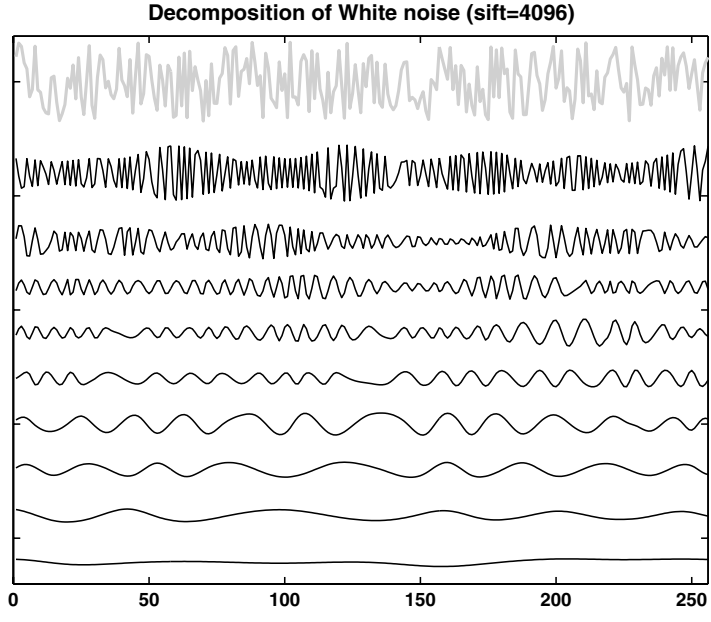


Fig. 7. Decomposition of a white noise series using EMD with a sifting number 4096. The gray line is the original white noise and the black lines are the IMFs of this time series.

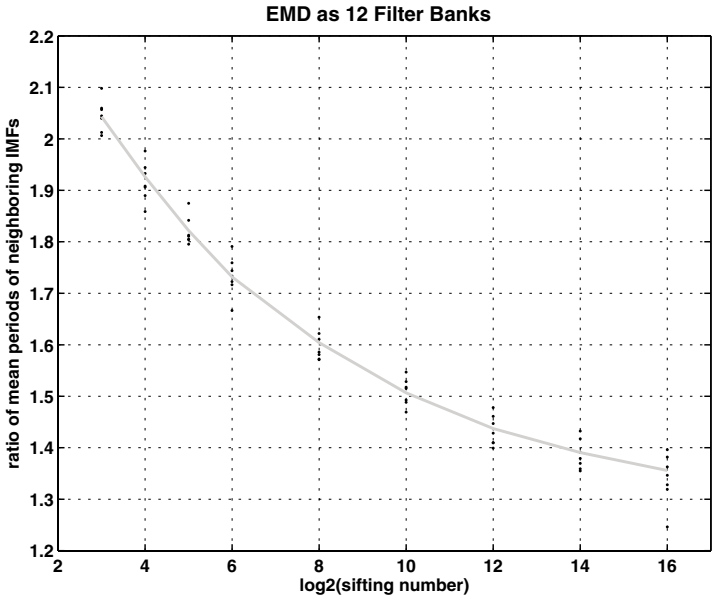


Fig. 8. The mean period ratio as a function of the sifting number of the decomposition. The individual mean period ratio for a given sifting number is plotted as black dots. The mean ratio for any given sifting number is plotted as the gray line.

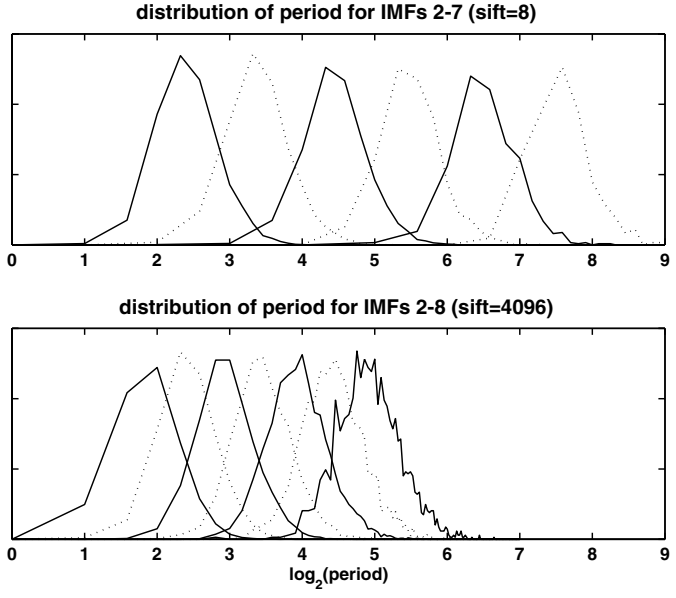


Fig. 9. The PDF of the period variability of IMF as a function of logarithm of period. In the upper panel, the PDFs for IMFs 2–7 in the case of a sifting number 8 is plotted from left to right; in the lower panel, the PDFs for IMFs 2–8 in the case of a sifting number 4096 is plotted from left to right.

Since EMD is an algorithm picking local high frequency oscillation first, the ratio of mean period cannot be a value smaller than 1. Therefore, we conjecture that the mean period ratio will asymptotically approach 1, as the sifting number increases to infinite.

In Figs. 6 and 7, we see that the local periods (defined as the distances between neighboring maxima) of any individual IMF, regardless of the sifting number, can vary significantly. This scale mixing problem is called "mode mixing." The mean period ratio as a function of the sifting number is shown in Fig. 8. Note that this plot does not provide information on the characteristics of the variation of the local period in any IMF. To gain insight into the period variation, the PDF of the period of an IMF as a function of the logarithm of period is plotted in Fig. 9. The noticeable fluctuations of the PDF for later IMFs (on the right-hand side of Fig. 9) are mainly caused by the small number of oscillation events for a given white noise of limit length. From Fig. 9, one concludes that the PDF of the period variation in the domain of logarithm of period is approximately an invariant, regardless of whether the mean period ratio decreases or the sifting number increases.

## 4. Discussions and Summary

In previous sections, based on numerical results, we conjectured that the EMD can behave like a filter bank having a mean filter ratio from 2 (dyadic) to 1 as the sifting number changes from a small number to infinity. By considering the mean period of an IMF in the high sifting number limit as the period for a trigonometric function, it is argued that FT can be recognized as a special case of EMD when the sifting number for EMD goes to infinity.

The results obtained in this study provide some insight into ways to optimize the EMD algorithm. Although the EMD method and its variant, the EEMD, have shown their usefulness in many applications, the empirical nature of the method has left crucial questions unanswered. One of them is how to determine when to stop sifting. Although an exact answer to this question may be out of our reach, we can design various stoppage criteria to optimize particular properties of the input data. As shown in Wu and Huang (2009), fixing the sifting number to low number in the EMD is the key to keep the EMD temporally local. However, the question of how to pick an appropriate sifting number is not answered. Through this study, we can select the optimal number of siftings: if we wish the EMD to be similar to an adaptive dyadic filter bank, the sifting number should be around 10. In such a sense, this study also provides some justification for the selection of the fixed sifting number 10 for the EMD algorithm.

During the preparation of this paper, Wang *et al.* (2010) proved that the infinite number of sifting results in the amplitude of IMF of any data being a straight line when the natural cubic spline is used to fit maxima and minima to obtain upper and lower envelopes of an IMF. The proof of Wang *et al.* (2010) is generalized in the appendix. While these proofs partly explained the numerical observations reported

in this paper, they also imply that the sifting process may not be an optimized approach for adaptive and local data analyses and the current EMD/EEMD algorithm may be *ad hoc*; and other generalized mathematical approaches need to be developed. Indeed, there have been progresses in the developments of mathematical alternatives to the EMD [Daubechies *et al.* (2009); Hou *et al.* (2009)]. These latter mathematical developments, undoubtedly, will serve as trail blazers to gain full mathematical understandings of EMD and to build more powerful tools for applications.

## Acknowledgments

The authors are grateful for Profs. I. Daubechies of Princeton University and T. Y. Hou of California Institute of Technology for their encouragements, suggestions, and revisions of the manuscript. ZW and NEH were sponsored by the NSF of USA grant ATM-0917743, Federal Highway Administration of USA grant DTFH61-08-00028, and grants from NSC of Republic of China, NSC95-2119-M-008-031-MY3, NSC97-2627-B-008-007, and from a grant from NCU, NCU 965941.

## Appendix: EMD with Envelope Fitting Using a Spline

In this appendix, we will prove that the strict symmetry requirement of upper and lower envelopes with respect to zero line for an IMF, which is obtained through the sifting process of EMD, results in the upper (lower) envelope being a single polynomial of $k$th order over the whole temporal domain of data if the spline selected to fit the local maxima (minima) is $k$th order. This proof follows closely and is a generalization of the proof of Wang *et al.* (2010) that a cubic natural spline envelope fitting to define upper and lower envelopes results in two symmetric straight line envelopes for a discrete time series whose local extrema are sparsely distributed (i.e., between two neighboring local extrema, there are at least two non-extrema data points). We will also note that the constraint of sparsely distributed extrema in Wang *et al.* (2010) is excessive and unnecessary.

The proof, which uses Fig. A.1 to illustrate, is extremely simple. Suppose we select a $k$th order ($k$ can be any natural number) spline for the EMD sifting and an IMF whose upper and lower envelopes are perfectly symmetric with respect to zero line is obtained after a certain large number of sifting. Since the spline is a defined piecewise by polynomials, we use $L_i(t)$ to represent the piecewise polynomial of the spline between two consecutive minima of the IMF at $t_{L,i-1}$ and $t_{L,i}$, $L_{i+1}(t)$ the piecewise polynomial between two consecutive minima of the IMF at $t_{L,i}$ and $t_{L,i+1}$, and $U_i(t)$ the piecewise polynomial between two consecutive maxima of the IMF at $t_{U,i-1}$ and $t_{U,i}$. Since the upper envelope and the lower envelope are perfectly symmetric with respect to the zero line, $L_i(t)$ must be $-U_i(t)$ between $t_{U,i-1}$ and $t_{L,i}$. Similarly, $L_{i+1}(t)$ must be $-U_i(t)$ between $t_{L,i}$ and $t_{U,i}$. Therefore, $L_i(t)$ and $L_{i+1}(t)$ must share the same polynomial expression as $-U_i(t)$. This proved that the neighboring piecewise polynomials must have the same polynomial expression.

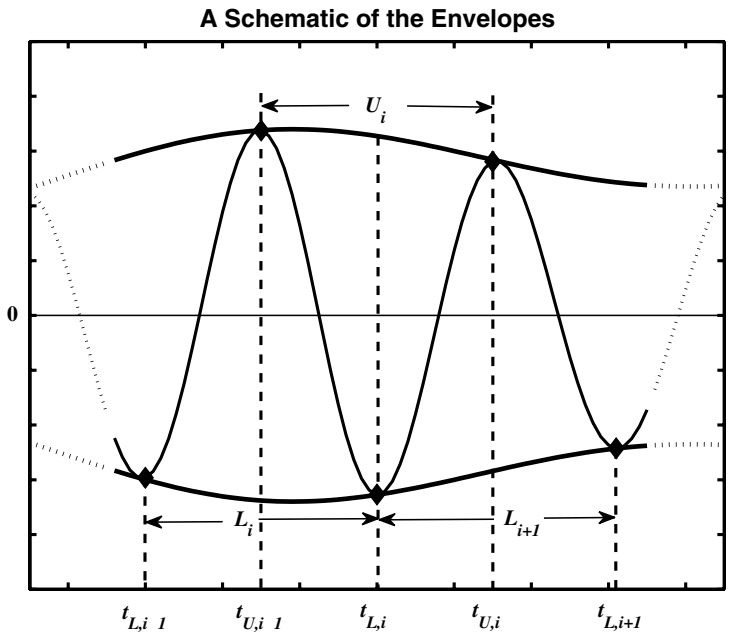


Fig. A.1. The schematic of an IMF and its envelopes.

Since $i$ is arbitrary, all piecewise polynomials between two consecutive minima must share the same polynomial expression; and thereby the piecewise spline for the lower envelope degenerates to a single polynomial over the whole temporal domain of the IMF. In the same way, we can prove that the spline for the upper envelope degenerates to a single polynomial of over the whole temporal domain, which is also the same $k$th polynomial for the upper envelope but with the opposite sign.

If a natural cubic spline is selected for the fitting of the envelopes in the EMD sifting, just as in the most EMD algorithms in practical use and in Wang *et al.* (2010), the second order derivatives of the upper (lower) spline fitted envelope at two ends of the IMF are set to zero. For a third-order polynomial, these boundary conditions make the coefficients of the quadratic and cubic terms of the polynomial being zero, degenerating the upper and lower envelopes into the same straight line but with opposite sign as Wang *et al.* (2010) proved. When higher order polynomials are used in EMD, what the global domain polynomial degenerates to is determined by the boundary conditions set for the splines.

Finally, we point out that the sparseness requirement in Wang *et al.* (2010) is not necessary. In the above proof, we did not specifically consider the spline fitting in the case of discrete series; and the proof is in general for the continuous functions. A following question is whether or not the above proof would still work for the discrete case. Since our arguments in the above proof used the polynomials

between a pair of neighboring extrema (which we call hereafter as "the half piecewise polynomial), whether or not the half piecewise polynomial can be uniquely determined needs to be clarified. When a maximum (minimum) is followed immediately by a minimum (maximum) in the discrete case without any other sampled temporal locations, two values [e.g., the maximum (minimum) and the mirrored point of its neighboring minimum (maximum)] would not be enough to uniquely determine the half piecewise polynomial. For this reason, Wang *et al.* (2010) proposed the sparseness condition for the distribution of extrema: there must be at least two more sampled temporal locations between two neighboring extrema. However, this sparseness is not necessary; in the case of the symmetric envelopes, the half piecewise polynomial is not independently determined, rather, the determination of the half piecewise polynomial has already implicitly used one extrema value immediately ahead of it and one extrema value immediately after it.

## References


Daubechies, I., Lu, J. and Wu, H.-T. (2009). Synchrosqueezed wavelet transforms: A tool for empirical mode decomposition. arXiv:0912.2437v1 [math.NA], http://arxiv.org/abs/0912.2437.

Flandrin, P., Rilling, G. and Gonçalves, P. (2004). Empirical mode decomposition as a filterbank. *IEEE Signal Proc. Lett.*, **11**: 112–114.

Flandrin, P. and Gonçalves, P. (2004). Empirical mode decompositions as data-driven wavelet-like expansions. *Int. J. Wavelets, Multiresolut. Inf. Process.*, **2**: 477–496.

Flandrin, P., Gonçalves, P. and Rilling, G. (2005). EMD equivalent filter bank, from interpretation to applications. in *Hilbert-Huang Transform and Its Applications*, Eds. N. E. Huang and S. Shen, World Scientific, Singapore, pp. 57–74.

Hou, T. Y., Yan, M. P. and Wu, Z. (2009). A variant of the EMD method for multiscale data. *Advances in Adaptive Data Analysis*, **1**: 483–516.

Huang, N. E., Shen, Z., Long, S. R., Wu, M. C., Shih, E. H., Zheng, Q., Tung, C. C. and Liu, H. H. (1998). The empirical mode decomposition and the Hilbert spectrum for nonlinear and non-stationary time series analysis. *Proc. Roy. Soc. Lond.*, **454A**: 903–993.

Huang, N. E., Shen, Z. and Long, S. R. (1999). A new view of nonlinear water waves — The Hilbert spectrum. *Ann. Rev. Fluid Mech.*, **31**: 417–457.

Huang, N. E., Wu, M. L., Long, S. R., Shen, S. S., Qu, W. D., Gloersen, P. and Fan, K. L. (2003). A confidence limit for the Empirical Mode Decomposition and Hilbert Spectral Analysis. *Proc. Roy. Soc. Lond.*, **459A**: 2317–2345.

Huang, N. E. and Attoh-Okine, N. O. (Ed.) (2005). *Hilbert-Huang Transforms in Engineering*, CRC Taylor and Francis Group, 313 pp.

Huang, N. E. and Shen, S. S. P. (Ed.) (2005). *Hilbert-Huang Transform and Its Applications*, World Scientific, Singapore, 311 pp.

Huang, N. E. and Wu, Z. (2008). A review on Hilbert-Huang Transform: the method and its applications on geophysical studies. *Rev. Geophys.*, **46**: RG2006, doi:10.1029/2007RG000228.

Huang, N. E., Wu, Z., Long, S. R., Arnold, K. C., Blank, K. and Liu, T. W. (2009). On instantaneous frequency. *Adv. Adapt. Data Anal.*, **1**: 177–229.

Rilling, G., Flandrin, P. and Gonçalvès, P. (2003). On empirical mode decomposition and its algorithms. *IEEE-EURASIP Workshop on Nonlinear Signal and Image Processing NSIP-03*, Grado (I).

Shen, S. P., Shu, T., Huang, N. E., Wu, Z., North, G. R., Carl, T. R. and Easterling, D. R. (2005). HHT analysis of the nonlinear and non-stationary annual cycle of daily surface air temperature data. In *Hilbert-Huang Transform: Introduction and Applications*, pp. 187–210, Ed. N. E. Huang and S. S. P. Shen, World Scientific, Singapore, 311 pp.

Wang, G., Chen, X., Qiao, F., Wu, Z. and Huang, N. E. (2010). On intrinsic mode function. *Adv. Adapt. Data Anal.*, **2**: 277–293.

Wu, Z. and Huang, N. E. (2004). A study of the characteristics of white noise using the empirical mode decomposition method. *Proc. Roy. Soc. Lond.*, **460A**: 1597–1611.

Wu, Z. and Huang, N. E. (2005). Statistical significant test of intrinsic mode functions. In *Hilbert-Huang Transform: Introduction and Applications*, pp. 125–148, Eds. N. E. Huang and S. S. P. Shen, World Scientific, Singapore, 311.

Wu, Z., Huang, N. E, Long, S. R. and Peng, C.-K. (2007). On the trend, detrending, and the variability of nonlinear and non-stationary time series. *Proc. Natl. Acad. Sci. USA*, **104**: 14889–14894.

Wu, Z. and Huang, N. E. (2009). Ensemble empirical mode decomposition: A noise-assisted data analysis method. *Adv. Adapt. Data Anal.*, **1**: 1–41.

Wu, Z., Huang, N. E. and Chen, X. (2009). The multi-dimensional ensemble empirical mode decomposition method. *Adv. Adapt. Data Anal.*, **1**: 339–372